Journal of Inclusion Phenomena and Molecular Recognition in Chemistry **10**: 453–469, 1991.

Spectroscopic Studies on the Interaction between Acridine Orange and Bile Salts*

E. CHIESSI #
Dipartimento di Chimica, Università di Roma 'La Sapienza', P. le A. Moro 5, 00185 Rome, Italy.

M. D'ALAGNI
Dipartimento di Chimica, Università di Roma 'La Sapienza', P. le A. Moro 5, 00185 Rome, Italy, and *Centro di Studio per la Chimica dei Recettori e delle Molecole Biologicamente Attive del C.N.R., c/o Istituto di Chimica, Università Cattolica, Largo F. Vito 1, 00168 Rome, Italy.*

G. ESPOSITO
Eniricerche S.p.A., 00015 Monterodondo, Rome, Italy.

and

E. GIGLIO**
Dipartimento di Chimica, Università di Roma 'La Sapienza', P. le A. Moro 5, 00185 Rome, Italy.

(Received: 16 October 1990; in final form: 20 February 1991)

Abstract. The structure of sodium deoxycholate (NaDC) micellar aggregates has been previously reported to be helical, and two helical models have been proposed for the micellar aggregates of sodium taurodeoxycholate (NaTDC). Here we report NMR and UV–VIS studies on the interaction between acridine orange (AO) and NaDC or NaTDC aqueous micellar solutions. AO is known to aggregate in aqueous solutions. The addition of NaDC or NaTDC causes the breaking of the AO aggregates, although the binding geometry of the two bile salts with AO seems to be slightly different. The cationic dye interacts mainly with the C_{18} and C_{19} methyl groups of the bile salt molecules. This result agrees with one of the two NaTDC helical models and with some of its possible aggregates, and confirms again the helical structure attributed to the NaDC micellar aggregates within the limits of the experimental conditions tested by us.

Key words. Sodium deoxycholate and taurodeoxycholate, acridine orange, micelle–probe interaction.

1. Introduction

WAXS, SAXS, EXAFS, NMR, ESR and CD measurements have enabled us to establish unequivocally that the structure of sodium and rubidium deoxycholate (NaDC and RbDC, respectively) micellar aggregates in aqueous solutions is helical [1–6]. An analogous study has been undetaken on sodium glycodeoxycholate (NaGDC) and taurodeoxycholate (NaTDC), compounds of remarkable biological interest since the bile salts in man are conjugated with glycine and taurine. Helical models have again been identified, but not yet conclusively proved, for NaGDC and NaTDC [7–9].

Present address: Dipartimento di Chimica, Università di Roma 'Tor Vergata', 00173 Roma, Italy.
*Devoted to Professor Giovannai Battista Marini Bettolo Marconi on the occasion of his 75th birthday.
**Author for correspondence.

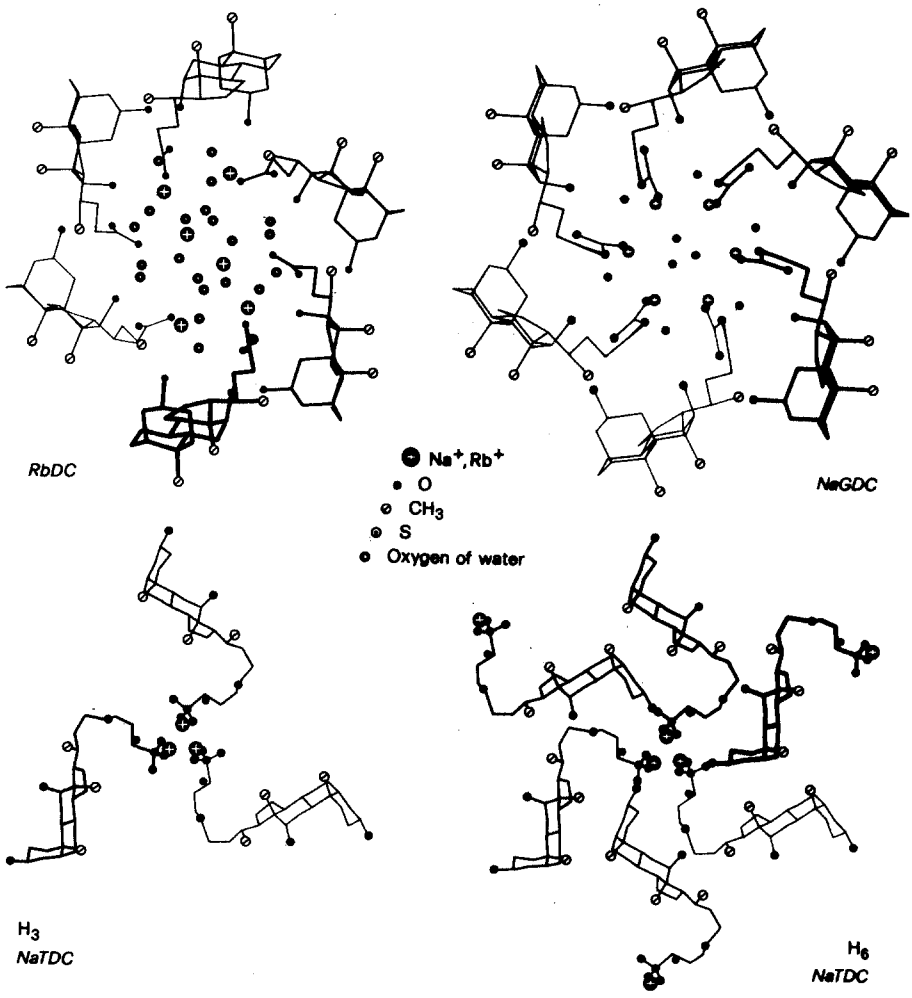

Fig. 1. View of the RbDC, NaGDC and NaTDC helices along the helical axis. A thicker anion is nearer to the observer. Two possible helices, $\mathbf{H}_3$ and $\mathbf{H}_6$, are shown for NaTDC. $\mathbf{H}_6$ is formed by two parallel spirals, shifted 7.1 Å along the helical axis, superimposed in projection.

The left-handed helix of NaGDC is very similar to those of NaDC and RbDC (Figure 1) with its lateral surface covered by nonpolar groups, such as the methyl groups C_{18} and C_{19} (Figure 2), and with its interior part filled with cations surrounded by water molecules. These helices are strongly stabilized by ion–ion interactions between cations and carboxylate ions, by ion–dipole interactions between cations and water molecules or hydroxyl groups, and by a close network of hydrogen bonds [10]. The solubility of the helices in water can be accounted for because the separation between two neighboring anions is such that the solvent molecules can approach the NaDC, RbDC and NaGDC polar groups through the lateral surface and near the end-monomers.

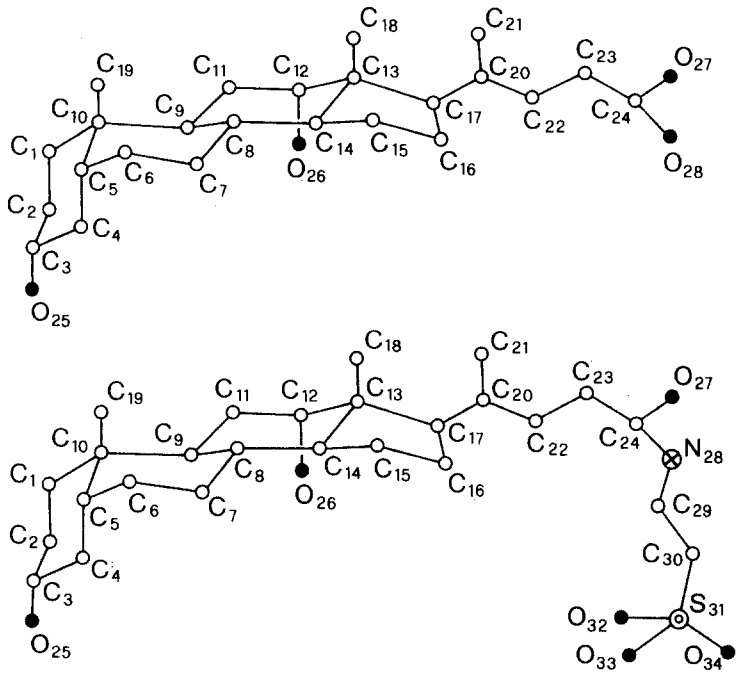

Fig. 2. Atomic numbering of the NaDC (top) and NaTDC (bottom) anions. The hydrogen atoms are omitted and referred in the text with the number of the parent carbon atoms.

Two possible 3_1 helices, indicated as $\mathbf{H_3}$ and $\mathbf{H_6}$ (Figure 1) or a system formed by the two helices in equilibrium, have been suggested for NaTDC micellar solutions [7, 8]. Their periodicity along the helical axis is 7.1 Å (t_h). The main interactions which stabilize the two helices are ion–ion, ion–dipole and hydrogen bonding [7]. $\mathbf{H_3}$ has three NaTDC molecules within t_h, a radius of approximately 16 Å, and SO_3^- groups, Na^+ ions and water molecules near the helical axis, whereas the O_{25} hydroxyls are the farthest groups from the helical axis. $\mathbf{H_6}$ can be obtained from $\mathbf{H_3}$ by inclusion within t_h of three more NaTDC molecules arranged with the O_{25} hydroxyls and the SO_3^- groups nearest to and farthest from the helical axis, respectively, and presents a radius of approximately 17 Å (the radius coincides with the longest distance of a NaTDC atom from the helical axis, excluding the hydrogen atoms). The lateral surface of both helices is covered by polar and nonpolar groups (Figure 1), the trilobate one of $\mathbf{H_3}$ being less polar than that of $\mathbf{H_6}$. Sedimentation and diffusion experiments seem to indicate that NaTDC micellar aggregates are highly hydrated [11], in agreement with the helical models showing, especially for the $\mathbf{H_3}$ one, a large empty space between two adjacent anions which can be filled with water molecules. Moreover, NaTDC aqueous electrolyte solutions have been studied as a function of NaTDC concentration, ionic strength and temperature by means of the SAXS technique [12]. The

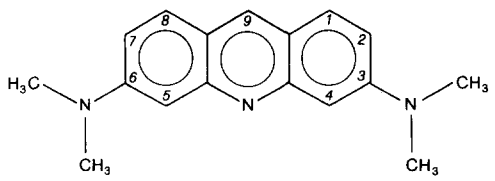

Fig. 3. Atomic numbering of AO. The hydrogen atoms are omitted and referred in the text with the number of the parent carbon atoms.

results agree with rod-like micellar aggregates of variable length and constant radius, about 18 Å. Thus, the shape is in agreement with that of the helical models as well as with the value of the radius, because a possible water of hydration can enlarge the cross section of the $\mathbf{H_3}$ and $\mathbf{H_6}$ helices [9].

Acridine orange (AO), a dye with no asymmetric centers (Figure 3), binds to both the random and α-helical conformations of poly-L- and poly-D-glutamic acid (L-PGA and D-PGA, respectively) over the pH range 4–7 [13, 14]. The optical rotatory dispersions of AO with the random L-PGA and D-PGA are almost identical with those of the polypeptides alone, whereas those of AO with the helical L-PGA and D-PGA are anomalous, with Cotton effects of opposite sign having an inflection point corresponding to the absorption maximum of the bound dye. Hence, the observed Cotton effects may serve as a simple and effective method for the determination of the helix sense [14].

Therefore, using CD, UV–VIS and NMR spectroscopic techniques, we decided to investigate the systems formed by AO with NaDC or NaTDC micellar aggregates in order to acquire more information on the structure of the NaTDC aggregates, using, for a useful comparison, the results obtained from the system AO-NaDC, containing micellar aggregates of known structure. Previously a CD study of the interaction between bilirubin-IXα and NaDC, RbDC, NaGDC and NaTDC micellar aggregates showed that the optically inactive bile pigment exhibits the same bisignate Cotton effect on binding to all these bile salts [9]. Since a reasonable explanation is that one of the two enantiomeric conformers of bilirubin interacts, at least preferentially, with the micellar aggregates, which must be chiral objects like the helices reported in Figure 1, bilirubin can be used as a 'helix detector'. AO could also provide the helical sense.

2. Experimental Section

2.1. MATERIALS

AO hydrochloride hydrate (Aldrich, 98%) was a rigorously purified zinc-free material. Its solutions were shielded from light in order to avoid photosensitized reactions. NaDC (Calbiochem) and NaTDC (Sigma) were recrystallized several times from the mixture of water and acetone. D_2O (100%) was purchased from Aldrich. NaCl (Merck, suprapur) was used.

2.2. PHYSICAL MEASUREMENTS

The CD measurements were performed by means of a JASCO J-500A spectropolarimeter at 20°C, calibrated with androsterone. Dry ultrapurified nitrogen was flushed before and during the experiments. pH was measured with a Radiometer (Copenhagen) Model 26 pH meter. The reported pH values in the NMR measurements are uncorrected pH meter readings obtained by the PM 62 Radiometer apparatus (Copenhagen) equipped with a combined glass microelectrode (Ingold).

Absorption spectra were measured in 1.0 and 0.1 cm cells at 25 and 30 ± 0.5°C by means of a Cary 219 spectropolarimeter.

^{1}H NMR measurements were performed at 400 MHz with a Bruker AM400 spectrometer by dissolving NaDC, NaTDC and AO hydrochloride in D_2O. The bile salt solutions were always 0.1 M. Typical conditions were: acquisition time 1.8 s in all the experiments; sweep width 3000 or 4500 Hz; digital resolution after Fourier transformation 0.36 or 0.55 Hz/point (depending on the sweep width); number of transients 40. Four hundred transients were collected for solutions at low concentrations. ^{13}C NMR measurements were carried out at 100.58 MHz with the same spectrometer and on the same samples employed for proton measurements (the spectrometer was equipped with a 5 mm heteronuclear probe). A sweep width of 21 000 Hz was always chosen, with an acquisition time of 0.3 s. Proton couplings were suppressed by WALTZ16 broad band decoupling, applied during acquisition and relaxation delay (0.2 s). The pulse flip angle was always kept around 40 degrees and 3000 transients were collected for each spectrum. Prior to Fourier transformation a Gaussian filtering function was applied to increase the sensitivity. The data were zero filled to 16 K points to achieve a final digital resolution of 2.6 Hz/point. The temperature was constant (25°C) throughout all the measurements. Chemical shifts were referred to internal TSP (sodium 2,2,3,3-tetradeuterio-3-(trimethylsilyl)propionate) both for carbon and proton spectra of bile salts. Because of possible association of the internal reference standard with bile salt micellar aggregates, a single reference measurement was performed for any series of spectra, keeping the spectrometer internal reference constant for the remaining spectra of the series. In order to prevent a similar problem with AO aqueous solutions without bile salts the relative spectra were run using dioxane as internal reference (3.759 ppm for TSP).

3. Results and Discussion

3.1. CD AND UV–VIS STUDY

CD spectra of NaDC and NaTDC micellar solutions about 0.1 M containing AO with concentrations up to 2.2×10^{-4} M showed no Cotton effects using quartz cells with a path length of 1.0 and 0.1 cm. Unfortunately, the increase of the AO concentration caused too high an optical density and, hence, we resorted to UV–VIS and NMR spectroscopies to investigate the bile salt-dye interactions.

It is well known that AO aggregates in aqueous solutions [15]. Its absorption spectrum in the visible region is characterized by three bands at about 490, 470 and 450 nm (α, β and γ band, respectively). Their location and intensity depend on the

AO concentration, the pH, ionic strength and temperature [15–17]. The maximum at the longer wavelength, favored by decreasing the AO concentration and pH and by increasing the temperature, was attributed to the presence of AO monomers. By contrast, the maxima at the shorter wavelengths arise with the opposite conditions, thus indicating the formation of dimers (β band) and of multimers (γ band) [15–17]. Since the association constant in the equilibrium $2\ AO \rightleftharpoons (AO)_2$ was found to correspond to a free energy of dimerization in aqueous solution at 17°C of $-25.1\ kJ\ mol^{-1}$, it was thought to be reasonable that the dye molecules aggregate by stacking on top of one another, held together mainly by dispersion forces [15]. However, Lamm and Neville showed later that the dimer spectrum of AO can be fitted by two different dimerization equilibria, one in agreement with that proposed by Zanker [15] and the other involving the formation of an anion [16].

There are some possible models of interaction between AO and PGA that could give rise to configurationally- or conformationally-induced Cotton effects of the dye [13]. Among these the model corresponding to a dye superhelix bound to the α-helix of PGA seems to be the most reliable. In fact, from UV–VIS and CD spectra it was inferred that in the L-PGA–AO complex the dye forms a left-handed superhelix around the right-handed α-helix of the polypeptide [18]. Since the induced Cotton effects of the dye are observed also at an amino acid residue-to-dye ratio of 1000 and above [13] and AO has a high stacking tendency [17], it is reasonable to suppose that the dye molecules of the superhelix occupy adjacent sites on the L-PGA α-helix in such a way as to be concentrated in short helical regions and to form multimers. Moreover, it was proposed that the shorter and longer axis of AO is probably orientated with respect to the L-PGA helical axis radially and at an angle within the range 0–45°, respectively [18].

The absorption spectrum of free AO in dilute aqueous solution is shown in Figure 4. When NaDC or NaTDC is added with a concentration below the critical micellar concentration (c.m.c.) the absorption decreases evenly in almost all the wavelength region, without significant shifts in the maximum positions, suggesting intermolecular interactions between AO and the anion which are stronger with NaTDC than with NaDC.

A few spectra of AO and NaDC are reported as typical examples in Figure 5. The increase of the AO concentration causes the formation of dimers and multimers and the disappearance of monomers (spectra A and D). The increase of ionic strength depresses the monomeric α band in favor of the β and γ association bands (spectra D and E), since the ionic repulsive interactions among positively charged AO molecules are more screened and the attractive van der Waals interactions acquire a greater weight. A remarkable change in the spectrum arises when NaDC micellar aggregates are present. The α monomeric band becomes predominant with a red shift in the absorption maximum of about 7 nm (spectra A and C, from 492 to 499 nm) and this effect appears much more in the presence of NaCl (spectra E and F). The results are consistent with a NaDC micelle—AO monomer interaction, which removes AO molecules from the dimers and multimers, and gives rise to a greater amount of monomer, taking into account both the free AO monomers in solution and those bound to the micelles. However, this interaction is clearly different from the one arising with the NaDC monomers, as can be inferred from

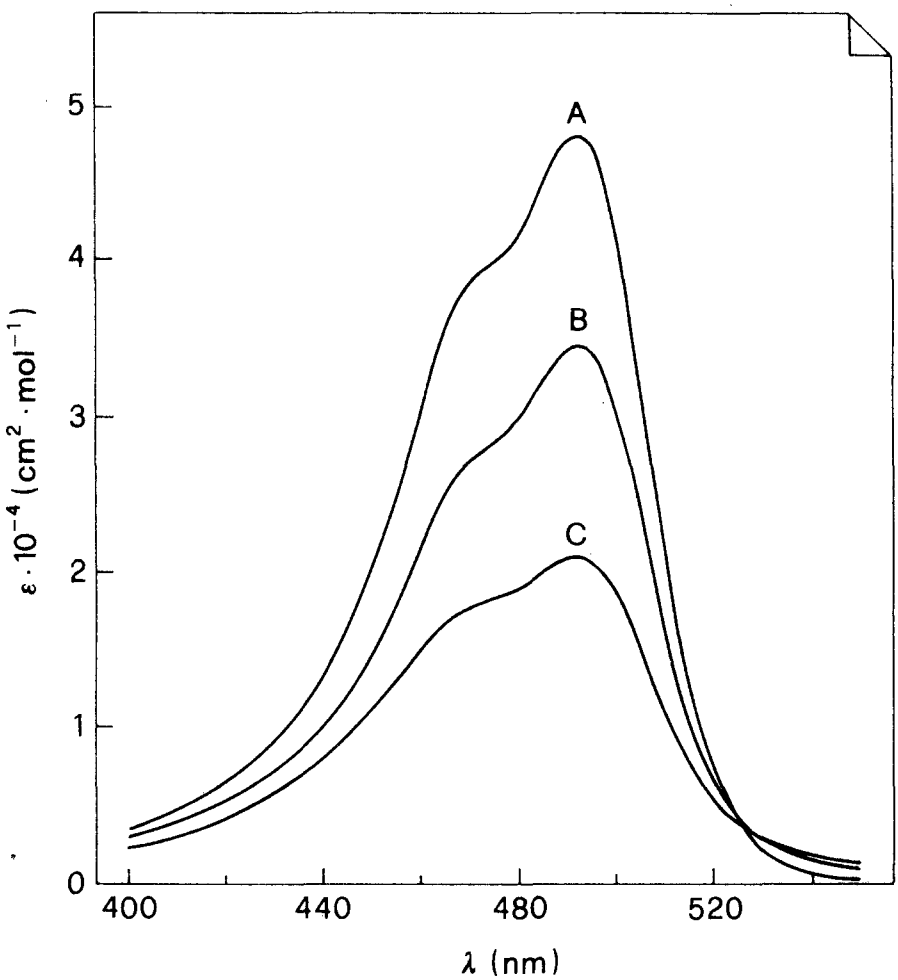

Fig. 4. Absorption spectra at 25°C of aqueous solutions of AO 2.3×10^{-5} M (A), with NaDC 7.4×10^{-4} M (B), and with NaTDC 9.4×10^{-4} M (C). Pathlength: 1 cm.

a comparison of spectra A, B and C, since when the NaDC concentration is below the c.m.c. the ratio of monomers/aggregates for the dye seems to be approximately equal to that observed in free AO.

NaTDC follows a trend similar to that of NaDC, with the same position of the wavelength maximum of the α band (499 nm). Spectrum D of Figure 6, for example, shows a strict similarity with spectrum F of Figure 5, suggesting that the dye-micelle interactions are of the same type for NaDC and NaTDC.

3.2. NMR STUDY

In order to obtain information on the binding sites of the bile salts, the dye–micelle systems were examined by ^{1}H and ^{13}C NMR spectroscopy, keeping the NaDC and NaTDC concentration constant at 0.1 M. Unfortunately, very small upfield shifts

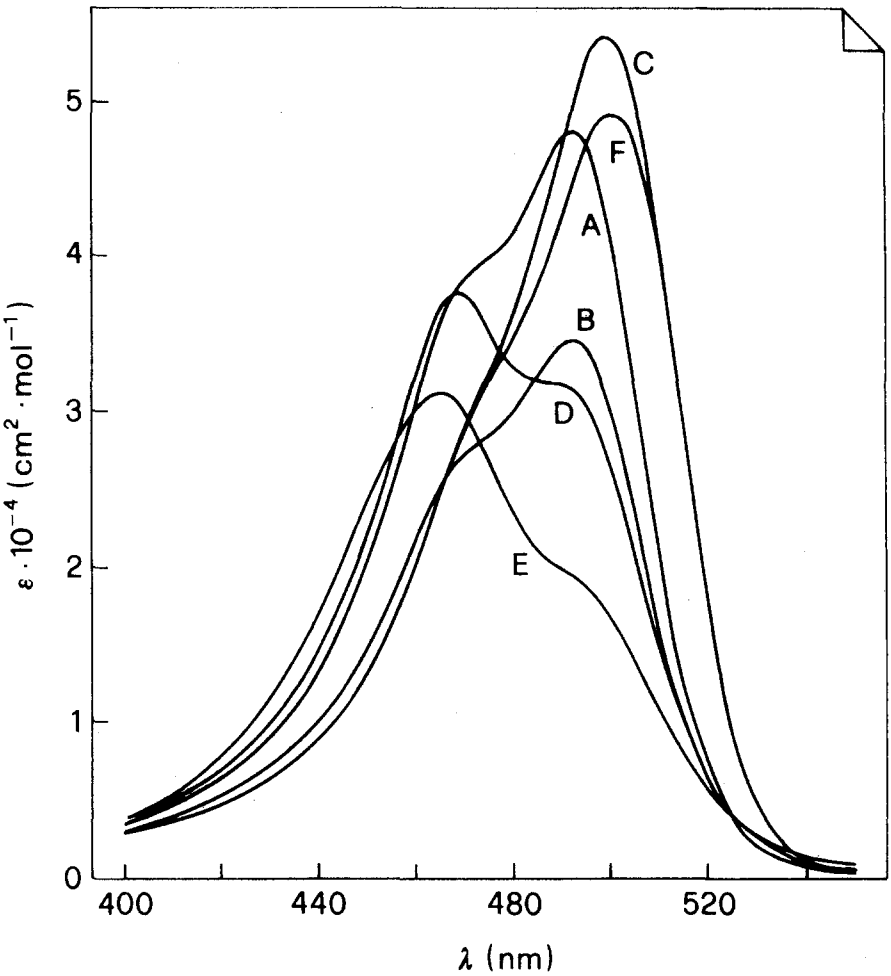

Fig. 5. Absorption spectra at 25°C of aqueous solutions of AO 2.3×10^{-5} M (A), with NaDC 7.4×10^{-4} M (B), and with NaDC 0.050 M (C), of AO 2.05×10^{-4} M (D), with NaCl 0.31 M (E), with NaDC 0.097 M and NaCl 0.31 M (F). Pathlength: 1 cm for A, B and C; 0.1 cm for D, E and F.

($\sim$0.02 ppm) are systematically observed for ^{13}C resonances only when the dye/bile salt molar ratio R is as high as possible (approximately 0.05) since above this value a precipitate is formed. Probably, the distances between the AO atoms and the carbons of the bile salts, owing to the intermediate hydrogen atoms, are sufficiently long to cause insignificant chemical shift variations.

More pronounced upfield shifts are observed for the NaDC and NaTDC protons which present a more suitable spatial proximity than the carbon atoms to the AO molecules (Figures 7 and 8). The chemical shift changes of the resolved signals generally increase on increasing R (Figure 8). They were assigned to the protons of C_{18} (Me_{18}), C_{19} (Me_{19}), C_{21} (Me_{21}), C_3 (H_3) and C_{12} (H_{12}) with resonances at 0.691, 0.909, 0.969, 3.592 and 4.023 ppm, respectively, for NaDC, and at 0.682, 0.907, 0.986, 3.595 and 4.010 ppm, respectively, for NaTDC (Figure 7). Moreover,

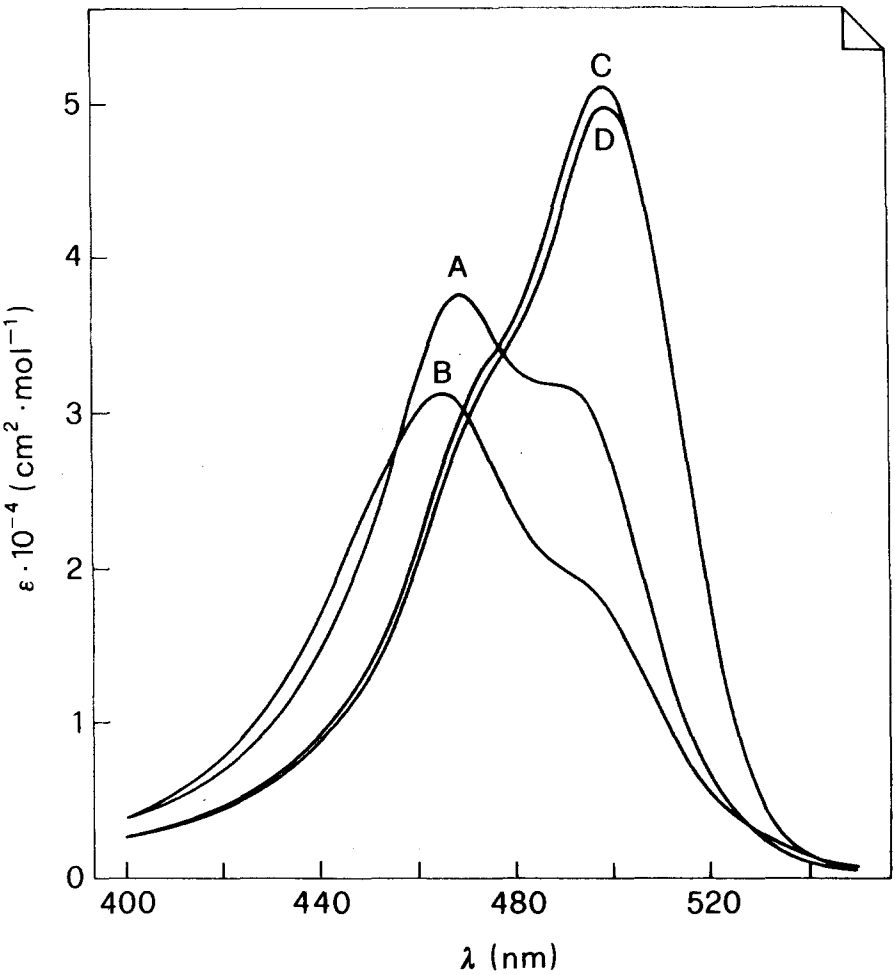

Fig. 6. Absorption spectra at 30°C of aqueous solutions of AO 2.21×10^{-4} M (A), with NaCl 0.32 M (B), with NaTDC 0.078 M (C), with NaTDC 0.118 M and NaCl 0.32 M (D). Pathlength: 0.1 cm.

the protons of C_{30} show resonances at 3.056 ppm and those of C_{29} at 3.543 ppm with a partial overlap with H_3, but they do not give rise to any significant chemical shift upon addition of AO. Again, C_{18} and C_{19} methyl groups together with H_{12}, belonging to the β face of the steroid molecule, undergo the largest upfield shifts [2, 4, 19], which are greater for NaDC than for NaTDC (Figure 8).

These results are in agreement with hydrophobic contacts involving mainly the NaDC helical methyl groups most protruding outside (Figure 1) and the AO molecules arranged with their aromatic rings approximately perpendicular to the C_{10}–C_{19} and C_{13}–C_{18} bonds, the $C_{18}\cdots C_{19}$ intramolecular distance being comparable with that between the centers of the two outermost AO rings, which can hook simultaneously to Me_{18} and Me_{19}. This model accounts for both the upfield shift of H_{12}, which is located close to Me_{18} and could experience the AO ring current, and the appreciably smaller Me_{21} and H_3 chemical shifts since these protons are remote

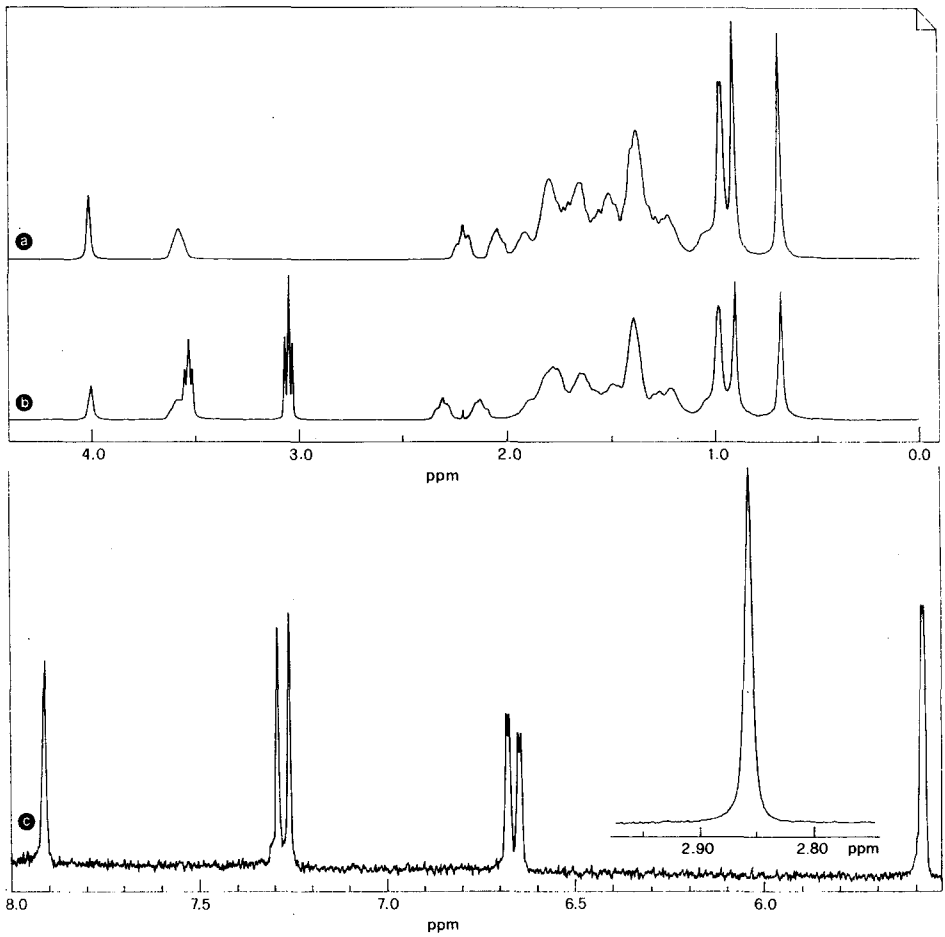

Fig. 7. ^{1}H 400–MHz spectra of NaDC 0.109 M (a), NaTDC 0.104 M (b), and AO 1.79×10^{-3} M (c) in D_2O.

and hardly approachable from AO. On the other hand, such a model also explains the failure to observe the induced Cotton effects if the dye superhelix scheme is invoked [18]. In fact, the AO molecules, with their ring planes almost parallel to the axis of the NaDC helices, randomly interact with Me_{18} and Me_{19}, occupy sites far from one another, and cannot take advantage of their stacking energy to form the superhelix.

The chemical shift variations of the NaTDC protons are generally smaller than those of NaDC (Figure 8). Plainly, a binding mode between AO and Me_{18}, Me_{19} and H_{12} of NaTDC, equal to the one proposed for NaDC, does not occur even though the dye molecules enter into the empty space of the trilobate $\mathbf{H_3}$ structure (Figure 1), filled by water molecules in aqueous solution [11, 12], owing to the steric hindrance of the folded back side chain. In this case an interaction with the C_{30} protons should occur, contrary to what can be expected from the constant values of their chemical shifts by varying the AO concentration. However, binding geometries, for example, involving the methyl groups belonging to NaTDC molecules,

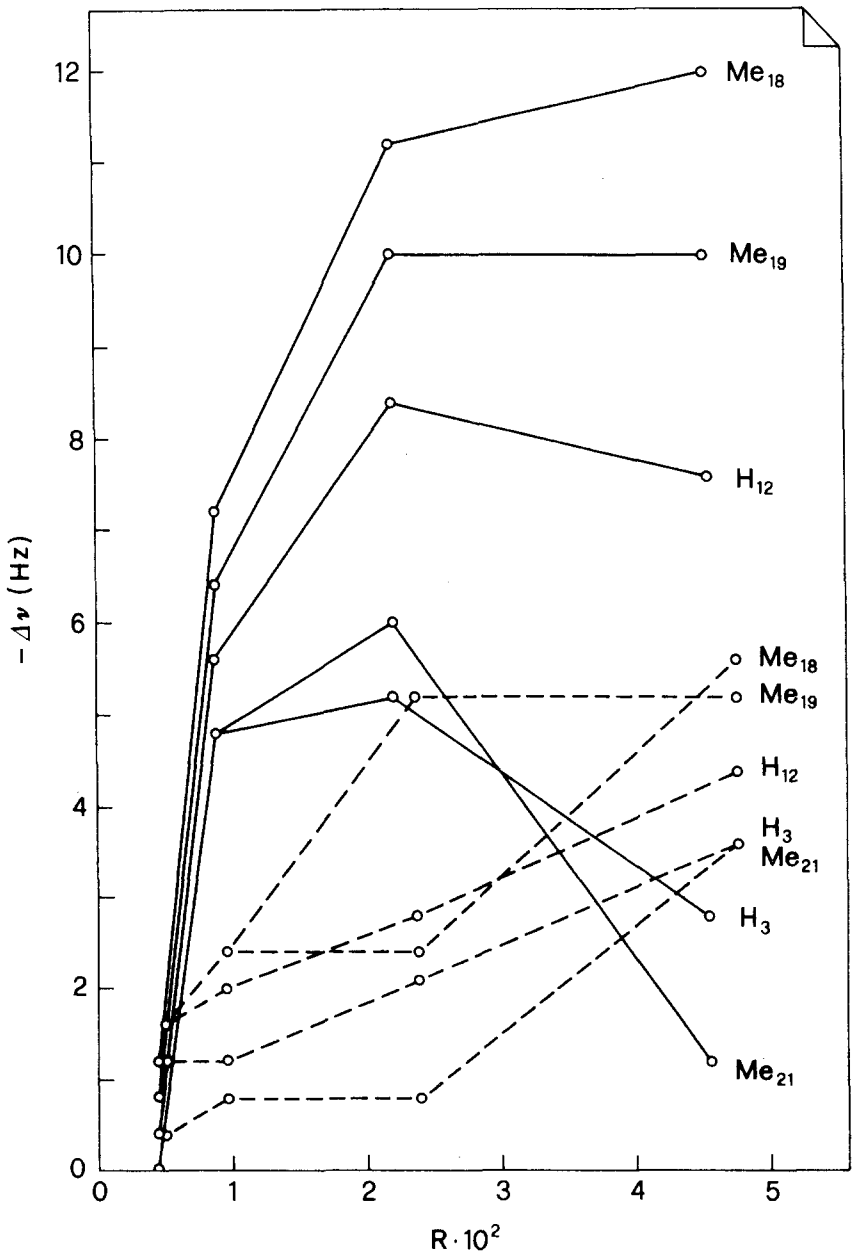

Fig. 8. Dependence of proton chemical shifts on R for NaDC (full lines) and NaTDC (broken lines). The bile salt concentration is 0.109 M.

shifted by t_h (7.1 Å) along the helical axis, may occur. As far as the $\mathbf{H_6}$ model is concerned, AO can approach some Me_{18} but not Me_{19} (Figure 1), so that a $\mathbf{H_6}\cdots$AO interaction of the abovementioned type seems to be ruled out.

The AO proton chemical shift changes (Figure 9), measured as a function of R, are much larger than those of the bile salt protons. The dye molecules bind to the

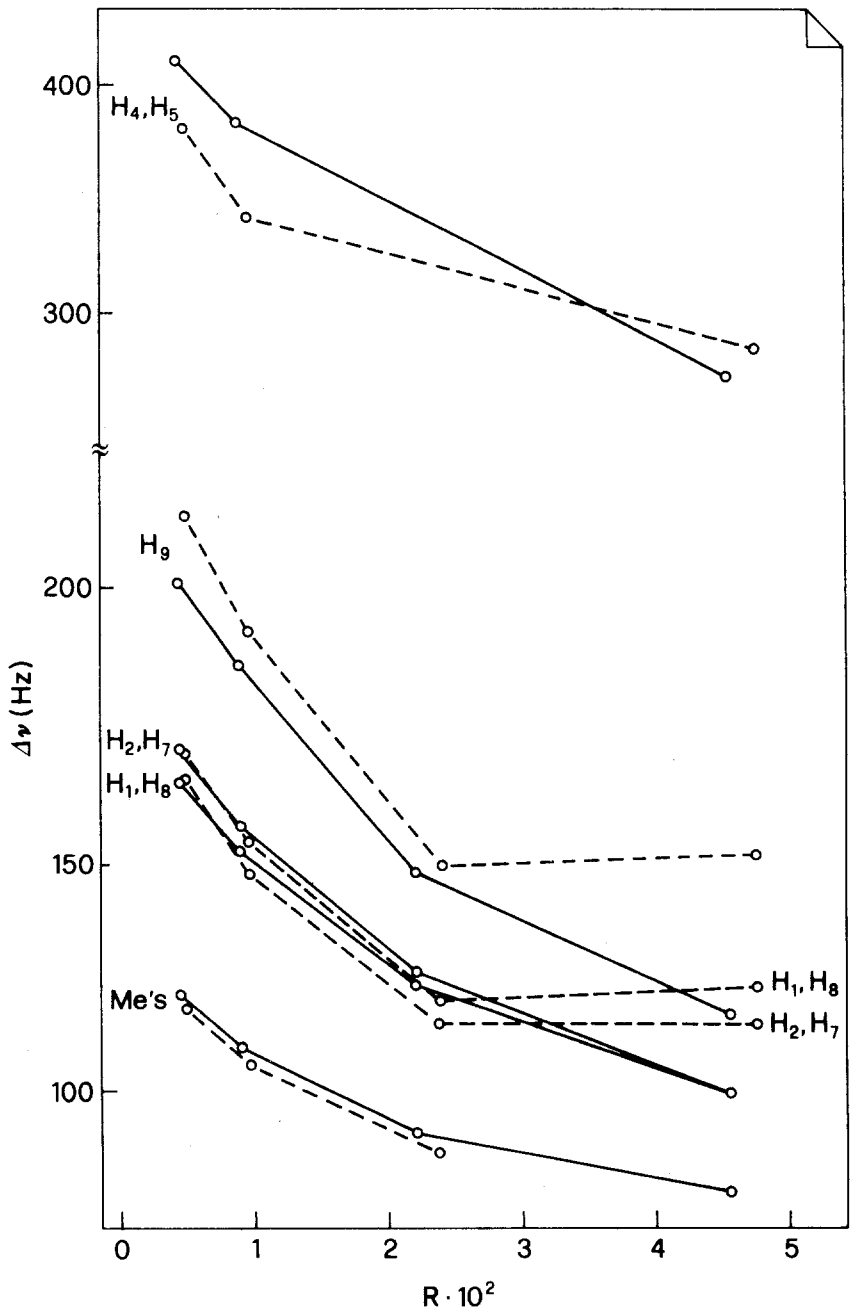

Fig. 9. Dependence of AO proton chemical shifts on R with NaDC (full lines) and NaTDC (broken lines). The bile salt concentration is 0.109 M. The chemical shift changes are referenced to SS.

micelles and simultaneously exist in solution as monomers, dimers and multimers. Hence, the chemical shifts are also influenced by the dye association, more favored in the NaDC solutions than in the NaTDC ones, which have a lower pH [15]. The proton resonances of an AO aqueous solution 2.0×10^{-3} M (hereafter indicated as SS, standard solution) are at 2.925, 5.663, 6.727, 7.343 and 7.976 ppm and correspond to the methyl groups, H_4 and H_5, H_2 and H_7, H_1 and H_8, and H_9, respectively (see Figure 3), as inferred from two-dimensional NOESY spectra (not reported here). The increase of the dye concentration causes upfield shifts (Figure 9) whose magnitude follows the sequence:

$$H_4,\ H_5 \gg H_9 > H_1,\ H_8 \sim H_2,\ H_7 > \text{Me's}$$

Thus, the side of the molecule containing H_4 and H_5 (nitrogen side) is appreciably more affected than that containing the remaining protons (carbon side). This is consistent with the ability of the nitrogen side to form hydrogen bonds or hydrogen bonds, ion–ion and ion–dipole interactions in the uncharged or charged molecule, respectively. These interactions can be conceived with the polar groups of the helix end-monomers for NaDC and of the helix end-monomers and lateral surface for NaTDC together with the polar groups of the bile salts monomers and of the solvent molecules. On the other hand, if the bile salt concentration is lower than the c.m.c., downfield shifts with respect to SS arise, very likely because types of binding, different from those occurring with the micelles, involve the bile salt charged heads and polar groups, as suggested also by the UV–VIS spectra.

The proton chemical shift changes of AO aqueous solutions without bile salt, referred to SS, depend on the dye concentration (Figure 10). Upfield shifts are recorded by increasing the concentration and, hence, the dye association. Their values follow the sequence:

$$H_4,\ H_5 \gg H_9 > H_1,\ H_8 \sim H_2,\ H_7 > \text{Me's}$$

already observed in the presence of NaDC or NaTDC (Figure 9). Clearly, the association phenomenon remarkably affects the chemical shifts, so that in a dye–bile salt solution the chemical shift changes are due both to the AO–bile salt interaction and to the dye association breaking, supported by the spectra of Figures 5 and 6.

The pH decrease plays a role in charging the dye, opposing its association. It was found [15] that the charged molecule prevails within the pH range 2–6, whereas there is an equilibrium between charged and uncharged molecules within the pH range 6–12. The behavior of the AO proton chemical shift changes, referred to SS, as a function of pH is reported in Figure 11 for two AO aqueous solutions. The one which is more dilute than SS generally shows small changes, probably because its concentration is too low. The other solution, with AO concentration comparable with SS, gives rise to greater changes, having a zigzag trend (Figure 11) which reflects both the association (upfield shifts, see Figure 10) and the discharging phenomenon. Its influence is supported by the greatest downfield shift changes of the nitrogen side protons H_4 and H_5, which experience more of the charging effects, as compared with those of the carbon side protons. The results, satisfactorily accurate, agree with those of Blears and Danyluk [20], obtained by means of a 60 MHz NMR spectrometer. They can be explained, for example, by a sandwich-

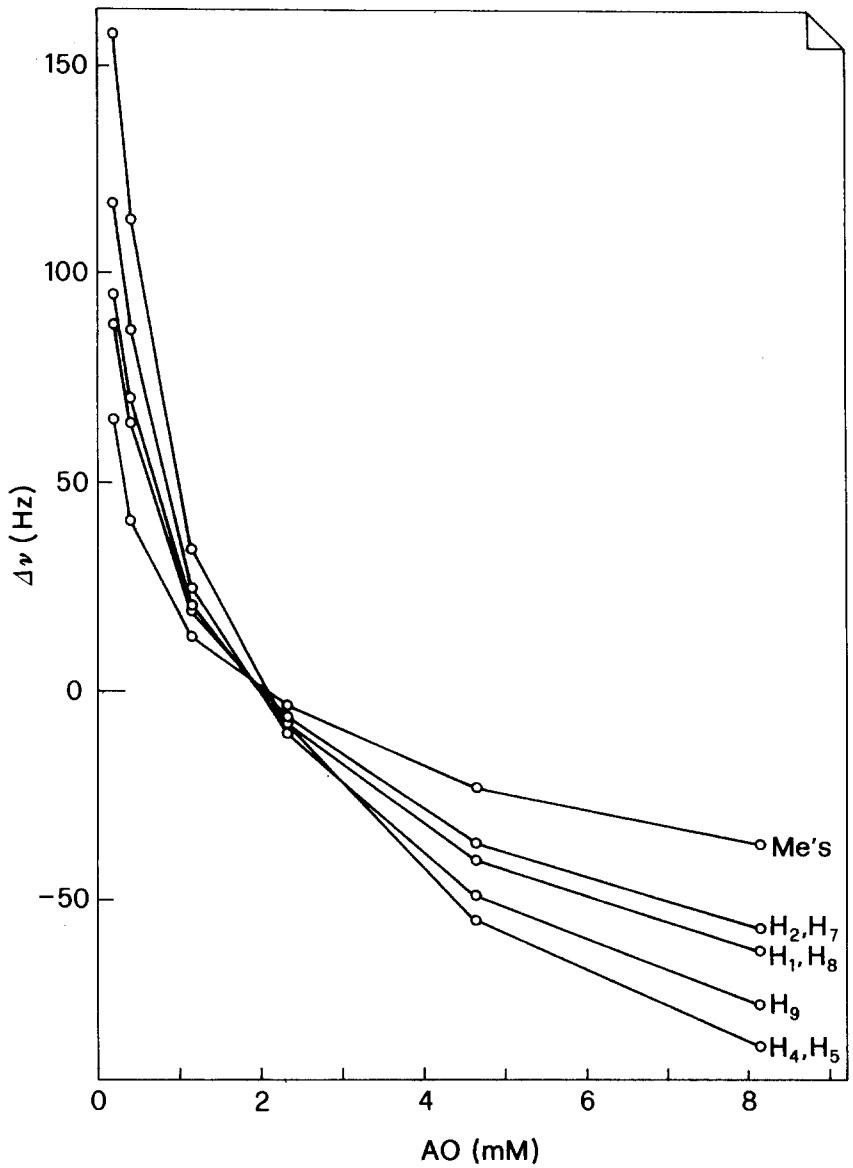

Fig. 10. Dependence of AO proton chemical shifts on the dye concentration. The chemical shift changes are referenced to SS.

like stacking of dimers, each formed by two molecules related by a center of inversion, as observed in the crystal structure of AO hydrochloride monohydrate or in that of AO hydroiodide [21]. In fact, these or similar models give rise to an overlap involving the nitrogen sides in the projection of a dimer along the normal to the AO molecular planes.

A last point deserves attention. Very recent SAXS measurements of NaTDC aqueous solutions, similar to those of NaDC [5], are in accordance with the

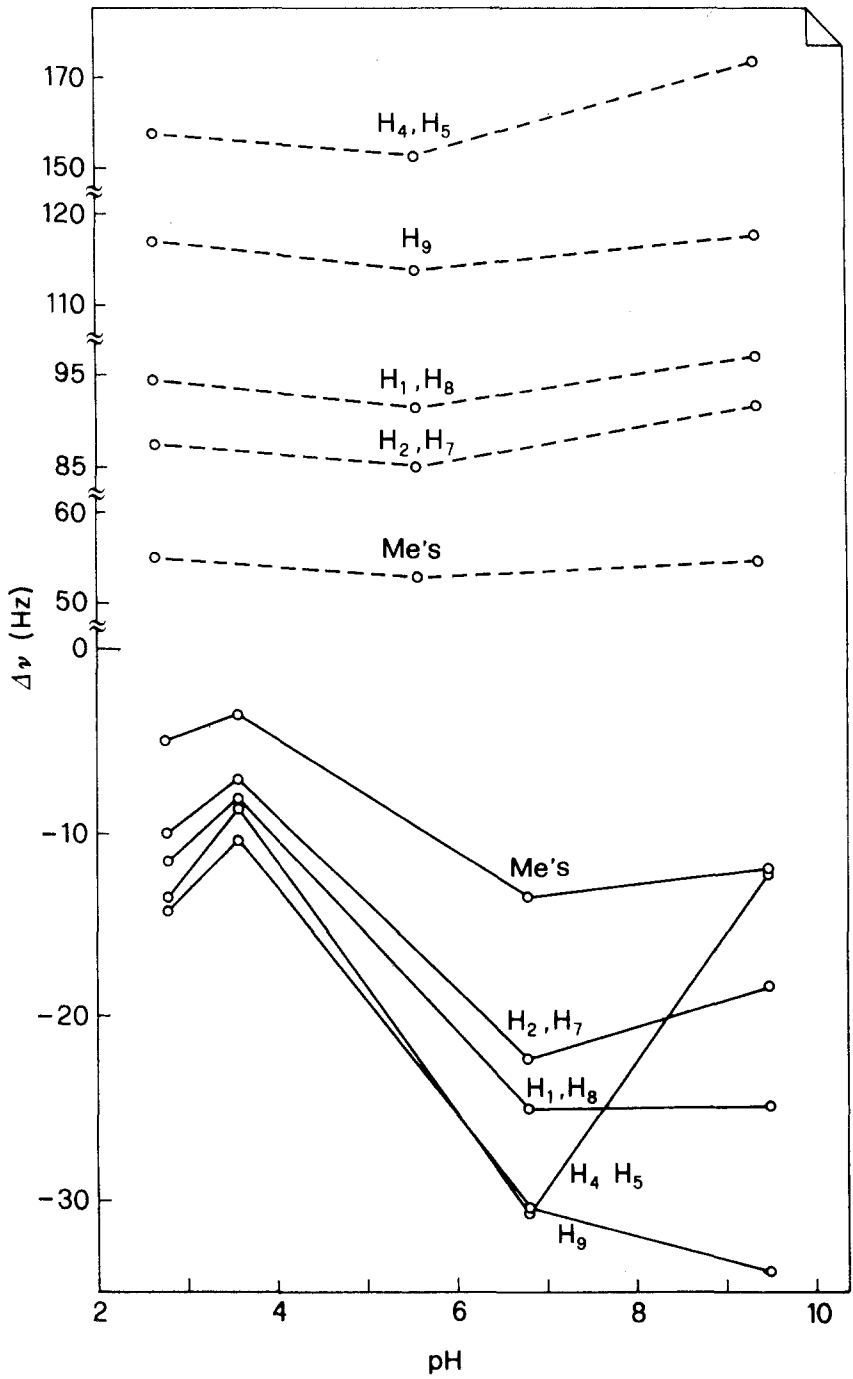

Fig. 11. Dependence of AO proton chemical shifts on pH. The AO concentration is 2.3×10^{-3} M (full lines) and 2.0×10^{-4} M (broken lines). The chemical shift changes are referenced to SS.

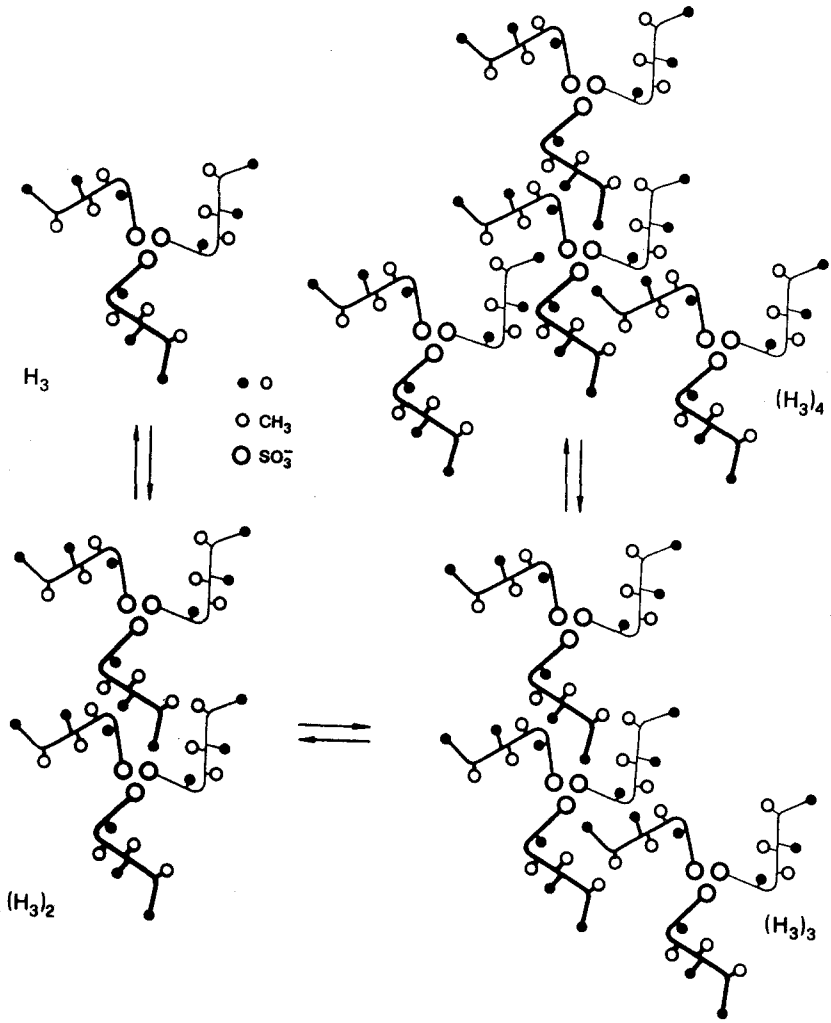

Fig. 12. Schematic drawing of the possible $\mathbf{H}_3$ aggregations for NaTDC. A thicker molecule is nearer to the observer.

existence of equilibria among species $\mathbf{H}_3$, $(\mathbf{H}_3)_2$, $(\mathbf{H}_3)_3$ and $(\mathbf{H}_3)_4$ and allow us to discard the $\mathbf{H}_6$ helix, thus confirming the NMR results of this work [unpublished results of E. Giglio, S. Morpurgo and N. V. Pavel]. Some possible $\mathbf{H}_3$ aggregates are represented schematically in Figure 12. They are found in the NaTDC crystal structure [7] and can interact with AO as a single $\mathbf{H}_3$ helix.

4. Conclusions

The main results of this study can be summarized as follows: (i) AO gives rise to association and charging phenomena by varying parameters such as concentration, pH and ionic strength. (ii) The dye-micelle interactions are hydrophobic, involve

mainly the C_{18} and C_{19} methyl groups of the bile salt molecules and favor the breaking of the AO association, increasing the amount of the AO monomers. Different interactions, probably involving polar groups, occur between AO and bile salt monomers. (iii) The bile salt binding sites agree with the observed NaDC helical model [5, 6, 10] and with the proposed NaTDC $\mathbf{H_3}$ helical model [7, 10] or with the $\mathbf{H_3}$ aggregates. The dye–micelle interaction geometries are different for NaDC and NaTDC. (iv) The dye–micelle binding geometry accounts for the failure of the Cotton effect, if it is due to the formation of a dye superhelix.

Acknowledgement

E.C. and E.G. wish to thank the Italian Ministero della Pubblica Istruzione and the Italian Consiglio Nazionale delle Ricerche – Progetto Finalizzato Chimica Fine e Secondaria – for financial support.

References

1. A. R. Campanelli, S. Candeloro De Sanctis, E. Giglio, and S. Petriconi: *Acta Crystallogr., Sect. C* **40**, 631 (1984).
2. G. Conte, R. Di Blasi, E. Giglio, A. Parretta, and N. V. Pavel: *J. Phys. Chem.* **88**, 5720 (1984).
3. M. D'Alagni, M. L. Forcellese, and E. Giglio: *Colloid Polym. Sci.* **263**, 160 (1985).
4. G. Esposito, A. Zanobi, E. Giglio, N. V. Pavel, and I. D. Campbell: *J. Phys. Chem.* **91**, 83 (1987).
5. G. Esposito, E. Giglio, N. V. Pavel, and A. Zanobi: *J. Phys. Chem.* **91**, 356 (1987).
6. E. Giglio, S. Loreti, and N. V. Pavel: *J. Phys. Chem.* **92**, 2858 (1988).
7. A. R. Campanelli, S. Candeloro De Sanctis, E. Giglio, and L. Scaramuzza: *J. Lipid Res.* **28**, 483 (1987).
8. M. D'Alagni, E. Giglio, and S. Petriconi: *Colloid Polym. Sci.* **265**, 517 (1987).
9. A. R. Campanelli, S. Candeloro De Sanctis, E. Chiessi, M. D'Alagni, E. Giglio, and L. Scaramuzza: *J. Phys. Chem.* **93**, 1536 (1989).
10. A. R. Campanelli, S. Candeloro De Sanctis, E. Giglio, N. V. Pavel, and C. Quagliata: *J. Incl. Phenom.* **7**, 390 (1989).
11. T. C. Laurent and H. Persson: *Biochim. Biophys. Acta* **106**, 616 (1965).
12. H. Matsuoka, J. P. Kratohvil, and N. Ise: *J. Colloid Interface Sci.* **118**, 387 (1987).
13. L. Stryer and E. R. Blout: *J. Am. Chem. Soc.* **83**, 1411 (1961).
14. E. R. Blout: *Tetrahedron* **13**, 123 (1961).
15. V. Zanker: *Z. Physik. Chem.* **199**, 225 (1952).
16. M. E. Lamm and D. M. Neville: *J. Phys. Chem.* **69**, 3872 (1965).
17. D. F. Bradley and M. K. Wolf: *Proc. Natl. Acad. Sci. U.S.A.* **45**, 944 (1959).
18. R. E. Ballard, A. J. McCaffery, and S. F. Mason: *Biopolymers* **4**, 97 (1966).
19. K. L. Puranam, S. Raghothama, and P. Balaram: *Biochim. Biophys. Acta* **922**, 67 (1987).
20. D. J. Blears and S. S. Danyluk: *J. Am. Chem. Soc.* **89**, 21 (1967).
21. C. A. Mattia, L. Mazzarella, V. Vitagliano, and R. Puliti: *J. Cryst. Spectrosc. Res.* **14**, 71 (1984).